

Studies of Thallium-Iridium Bonding

Alan L. Balch,* Francesco Neve, and Marilyn M. Olmstead

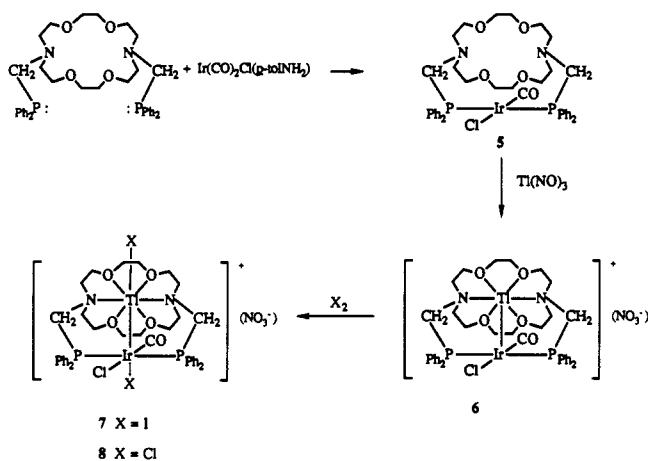
Contribution from the Department of Chemistry, University of California, Davis, California 95616. Received August 22, 1990

Abstract: New examples of complexes with Tl-Ir bonds have been prepared and structurally characterized. Treatment of $\text{Ph}_2\text{PCH}_2\text{N}[(\text{CH}_2)_2\text{O}(\text{CH}_2)_2\text{O}(\text{CH}_2)_2]_2\text{NCH}_2\text{PPh}_2$, crown-P₂, with $\text{Ir}(\text{CO})_2\text{Cl}(p\text{-toluidine})$ yields yellow (crown-P₂) $\text{Ir}(\text{CO})\text{Cl}$ which reacts with thallium(I) nitrate to give yellow-orange crystals of $[\text{Tl}(\text{crown-P}_2)\text{Ir}(\text{CO})\text{Cl}](\text{NO}_3)\cdot\text{CH}_2\text{Cl}_2$. These form in the triclinic space group *P*1 (No. 2) with $a = 11.350$ (4) Å, $b = 13.519$ (4) Å, $c = 15.022$ (4) Å, $\alpha = 97.64$ (2)°, $\beta = 101.20$ (3)°, $\gamma = 93.63$ (3)° at 130 K with $Z = 2$. Refinement of 6298 reflections and 243 parameters yielded $R = 0.070$, $R_w = 0.078$. The complex consists of a nearly planar $\text{Ir}(\text{CO})\text{ClP}_2$ unit and a thallium ion within the aza-crown portion. The Tl-Ir distance is 2.875 (1) Å. The presence of the thallium ion perturbs the electronic spectrum of the $\text{IrP}_2(\text{CO})\text{Cl}$ chromophore. The Tl-Ir complex has absorbance at 400 nm ($\epsilon = 17700$) and 500 nm ($\epsilon = 452$) at 23 °C in dichloromethane and strong emission at 580 nm in frozen dichloromethane at 77 K which is not observed when the sample is warmed to 23 °C. This Tl-Ir complex undergoes oxidative addition of iodine or chlorine (from iodobenzene dichloride) to form $[\text{TI}(\text{crown-P}_2)\text{Ir}(\text{CO})\text{ClI}]\text{NO}_3$ or $[\text{ClTI}(\text{crown-P}_2)\text{Ir}(\text{CO})\text{Cl}_2](\text{NO}_3)$. These show significant increases in $\nu(\text{CO})$ and $^2J(\text{Tl},\text{P})$ that are consistent with oxidation. As a model for the formation of these oxidation products which should have Tl-Ir single bonds, the structure of $(\text{CH}_3\text{CO}_2)_2\text{Tl}(\mu\text{-O}_2\text{CCH}_3)\text{Ir}(\text{CO})(\text{PPh}_3)_2(\text{O}_2\text{CCH}_3)\text{-CHCl}_3$ has been determined. Colorless crystals form in the monoclinic space group *P*2₁/*c* (No. 14) with $a = 10.815$ (3) Å, $b = 22.909$ (8) Å, $c = 21.582$ (7) Å, $\beta = 118.63$ (2)° at 130 K with $Z = 4$. Refinement of 3961 reflections with 296 parameters yielded $R = 0.063$, $R_w = 0.059$. The structure has a short Tl-Ir bond (2.611 (1) Å) with an acetate ion bridging the Tl-Ir unit. Two chelating acetate ligands are bound to the thallium while a terminal monodentate acetate is bound to iridium, whose coordination sphere is completed by a terminal carbonyl group and the pair of trans triphenylphosphine ligands. Thus all three common modes of acetate coordination are present in one compound. These structures are compared to that of $\text{Ir}_2(\text{TiNO}_3)(\text{CO})_2\text{Cl}_2(\mu\text{-Ph}_2\text{PCH}_2\text{As}(\text{Ph})\text{CH}_2\text{PPh}_2)_2$. The thallium atoms in these complexes show considerable variation in coordination number and angular ligand distribution, while the iridium atoms have rectilinear coordination. The bonding within the Tl-Ir units is discussed.

Introduction

Examples of transition-metal-thallium bonding, particularly with Tl(I), are rare. Among the known, structurally characterized, thallium transition-metal complexes are a set of cluster anions, $[\text{Tl}_x\text{Fe}_y(\text{CO})_z]^{n-}$, prepared by Whitmire and co-workers.¹ These have Tl-Fe bonds and may have Fe-Fe bonds, but the Tl...Tl distances exceed those in elemental thallium. The structure of a related cluster, $[\text{Tl}\{\text{Ru}_6\text{C}(\text{CO})_{16}\}_2]^{-}$, has been reported.² Tl- $[\text{Mo}(\text{CO})_3(\eta^5\text{-C}_5\text{H}_5)]_3$ contains a planar thallium atom coordination by three molybdenum atoms.³ In contrast $\text{Tl}[\text{Co}(\text{CO})_4]$ is a salt with no direct Tl-Co bond.⁴ A number of other transition-metal carbonyl derivatives of thallium have been prepared, but these remain structurally uncharacterized.⁵ A novel polymer, $\{\text{AuTl}(\text{CH}_2\text{P}(\text{S})\text{Ph}_2)\}_n$, containing an alternating Au/Tl chain has been prepared and characterized by Fackler and co-workers.⁶ Within the chain there are two types of Au-Tl contacts: those which are bridged by two $\text{CH}_2\text{P}(\text{S})\text{Ph}_2$ ligands with distances of 2.959 (2) Å and those which are unbridged with slightly longer distances (3.003 (2) Å). Addition of thallium nitrate to $\text{K}_2\text{Pt}(\text{CN})_4$ produces molecular *trans*- $\text{Tl}_2\text{Pt}(\text{CN})_4$ with a six-coordinate structure that involves two Pt-Tl bonds.^{7,8} The Tl-Pt bond of $\text{Tl}_2\text{Pt}(\text{CN})_4$ has been "solubilized" with use of the recently de-

Scheme I



veloped hybrid ligand **1** (crown-P₂) that has been used to prepare the Pt-Tl bonded species **2**.⁹ A thallium ion caps a Pt₃ triangle in $[\text{TlPt}_3(\text{CO})_3(\text{PCy}_3)_3]^+$.¹⁰ In contrast to the simple molecular structure of $\text{Tl}_2\text{Pt}(\text{CN})_4$, $\text{Tl}[\text{Au}(\text{CN})_4]$ possesses a complex structure which involves both Tl/Au and Au/Au contacts in the 3.037 (4)–3.560 (1) Å range.¹¹ Charge transfer phenomena have been reported for the salt $\text{Tl}_3\text{Fe}(\text{CN})_6$.¹² The carboxylated-bridge complex $\text{PdTl}(\text{O}_2\text{CR})_5$ has been studied spectroscopically.¹³

Thallium(I) nitrate reacts with the metallomacrocycle $\text{Ir}_2(\text{CO})_2\text{Cl}_2(\mu\text{-dpma})_2$ (**3**, where dpma is bis(diphenylphosphino)methyl)phenylarsine) to form the luminescent adduct **4**.¹⁴ Some

(1) Whitmire, K. H.; Ryan, R. R.; Wasserman, H. J.; Albright, T. A.; Kang, S.-K. *J. Am. Chem. Soc.* **1986**, *108*, 6831. Whitmire, K. H.; Cassidy, J. M.; Rheingold, A. L.; Ryan, R. R. *Inorg. Chem.* **1988**, *27*, 1347. Cassidy, J. M.; Whitmire, K. H. *Inorg. Chem.* **1989**, *28*, 1432. Cassidy, J. M.; Whitmire, K. H. *Inorg. Chem.* **1989**, *28*, 1435.

(2) Ansell, G. B.; Modrick, M. A.; Bradley, J. S. *Acta Crystallogr.* **1984**, *C40*, 1315.

(3) Ibers, J. A.; Rajaram, J. *Inorg. Chem.* **1973**, *12*, 1313. King, R. B. *Inorg. Chem.* **1970**, *9*, 1936.

(4) Schussler, D. P.; Robinson, W. R.; Edgell, W. F. *Inorg. Chem.* **1974**, *13*, 153.

(5) Burlitch, J. M.; Theyson, T. W. *J. Chem. Soc., Dalton Trans.* **1974**, 828.

(6) Wang, S.; Fackler, J. P., Jr.; King, C.; Wang, J. C. *J. Am. Chem. Soc.* **1988**, *110*, 3308. Wang, S.; Garzon, G.; King, C.; Wang, J.-C.; Fackler, J. P., Jr. *Inorg. Chem.* **1989**, *28*, 4623.

(7) Nagle, J. K.; Balch, A. L.; Olmstead, M. M. *J. Am. Chem. Soc.* **1988**, *110*, 319.

(8) Ziegler, T.; Nagle, J. K.; Snijderes, J. G.; Baerends, E. J. *J. Am. Chem. Soc.* **1989**, *111*, 5631.

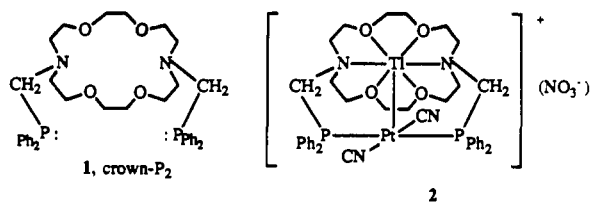
(9) Balch, A. L.; Rowley, S. P. *J. Am. Chem. Soc.* **1990**, *112*, 6139. (10) Ezomo, O. J.; Mingos, M. P.; Williams, I. D. *J. Chem. Soc., Chem. Commun.* **1987**, 924.

(11) Blom, N.; Ludi, A.; Bürgli, H.-B.; Tichy, K. *Acta Crystallogr., Sect. C: Struct. Commun.* **1984**, *C40*, 1767.

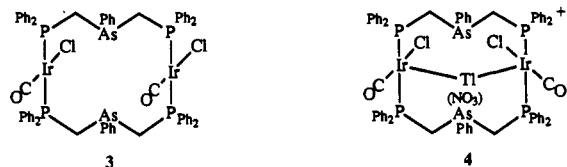
(12) Herbison-Evans, D.; Phipps, P. B. P.; Williams, R. J. P. *J. Chem. Soc.* **1965**, 6170.

(13) van Der Ploeg, A. F. M. J.; van Koten, G.; Vrieze, K. *Inorg. Chim. Acta* **1980**, *39*, 2536.

(14) Balch, A. L.; Nagle, J. K.; Olmstead, M. M.; Reedy, P. E., Jr. *J. Am. Chem. Soc.* **1987**, *109*, 4123.



related complexes have been obtained by van Vliet and Vrieze from the reaction of thallium(III) compounds with Vaska-like iridium complexes.¹⁵



This situation is in distinct contrast to the behavior of the isoelectronic tin(II) where complexes of the $(\text{SnCl}_3)^-$ unit are commonplace throughout the platinum group metals.¹⁶ However, it is notable that there has been much less development of related behavior of related systems involving Tl(I), In(I), or Pb(II). Here we examine the preparation and structures of several Tl–Ir complexes and assess the nature of the iridium–thallium bonds in them.

Results

Synthetic Studies. These are summarized in Scheme I. Treatment of $\text{Ir}(\text{CO})_2\text{Cl}(p\text{-tolNH}_2)$ ($p\text{-tol}$ is $p\text{-toluidine}$) with crown- P_2 in toluene gives a yellow solution from which $(\text{crown-P}_2)\text{Ir}(\text{CO})\text{Cl}$ (**5**) was isolated as a yellow solid by evaporation and addition of diethyl ether in 77% yield. The air-sensitive complex is soluble in acetone, toluene, chloroform, and dichloromethane but insoluble in diethyl ether and hydrocarbons. The $^{31}\text{P}\{^1\text{H}\}$ NMR spectrum shows a singlet at 10.6 ppm in chloroform. The infrared spectrum shows $\nu(\text{CO})$ at 1957 cm^{-1} , which is in the range expected for a Vaska-like complex.¹⁷ Upon exposure to air, a cream-colored dioxygen adduct, $(\text{crown-P}_2)\text{Ir}(\text{O}_2)(\text{CO})\text{Cl}$, is formed with spectroscopic properties ($\nu(\text{CO}) = 2002\text{ cm}^{-1}$, $^{31}\text{P}\{^1\text{H}\}$ NMR -0.4 ppm) consistent with the formulation.^{17,18} Addition of dihydrogen to **5** yields a complex mixture of hydride-containing substances which have not been further studied.

Addition of solid thallium nitrate to a dichloromethane solution of $(\text{crown-P}_2)\text{Ir}(\text{CO})\text{Cl}$ yields yellow-orange crystals of $[\text{Tl}(\text{crown-P}_2)\text{Ir}(\text{CO})\text{Cl}](\text{NO}_3)$ (**6**) after removal of excess thallium nitrate and precipitation with diethyl ether. The infrared spectrum shows $\nu(\text{CO})$ at 1968 cm^{-1} (that is within the range of Ir(I) complexes)¹⁷ and $\nu(\text{NO})$ at 1347 cm^{-1} for the nitrate ion. The $^{31}\text{P}\{^1\text{H}\}$ NMR spectrum consists of a doublet at 18.7 ppm with $^2J(\text{Tl,P}) = 84\text{ Hz}$. For comparison $^2J(\text{Tl,P})$ is 41 Hz for the Pt/Tl complex **2**.⁹

The electronic absorption spectrum shows evidence of Tl–Ir bonding. Figure 1 compares the absorption spectra of $(\text{crown-P}_2)\text{Ir}(\text{CO})\text{Cl}$ (trace A) with that of $[\text{Tl}(\text{crown-P}_2)\text{Ir}(\text{CO})\text{Cl}](\text{NO}_3)$ (trace B). The spectrum in trace A is typical of complexes with the $\text{IrP}_2(\text{CO})\text{Cl}$ coordination unit.¹⁹ The changes seen on going from trace A to trace B are taken to reflect on the Tl–Ir bonding. The prominent absorption in the latter at 400 nm ($\eta = 19\,700\text{ M}^{-1}\text{ cm}^{-1}$) is assigned to the Tl–Ir chromophore with the weak feature at 500 nm ($\eta = 452$) (which is expanded four times in the inset) taken as its spin-forbidden counterpart. Complex **6** is luminescent in a frozen dichloromethane solution at 77 K. The emission spectrum obtained from excitation at 400 nm is shown

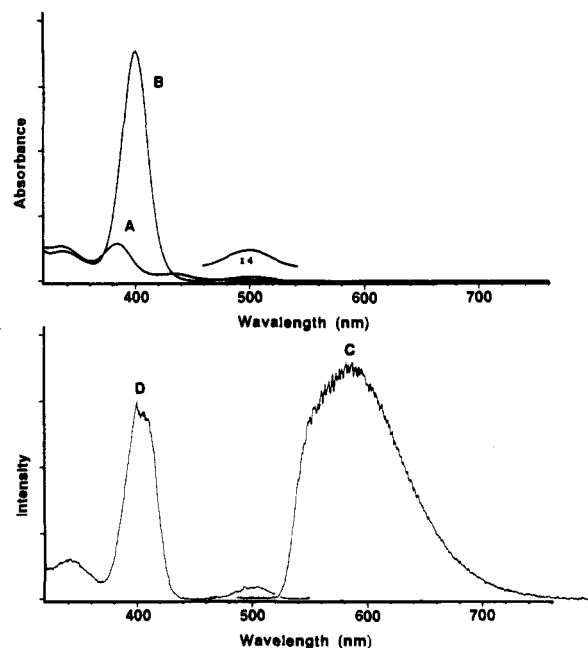


Figure 1. The electronic absorption spectra of (a) $(\text{crown-P}_2)\text{Ir}(\text{CO})\text{Cl}$ and (b) $[\text{Tl}(\text{crown-P}_2)\text{Ir}(\text{CO})\text{Cl}](\text{NO}_3)$ (**6**) in dichloromethane solution at $23\text{ }^\circ\text{C}$ and the uncorrected emission (C) and excitation (D) spectra for $[\text{Tl}(\text{crown-P}_2)\text{Ir}(\text{CO})\text{Cl}](\text{NO}_3)$ in frozen dichloromethane solution at 77 K .

in trace C of Figure 1. Trace D shows the excitation spectrum obtained for emission at 580 nm. This excitation spectrum matches the absorption spectrum (trace B). No emission is observed after the sample is warmed to $23\text{ }^\circ\text{C}$.

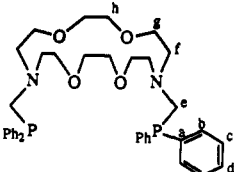
The Tl–Ir complex **6** has considerable chemical stability. Unlike the parent complex **5** it is stable to exposure to molecular oxygen both as a solid and in solution. Treatment of **6** with a 10-fold excess of 18-crown-6 has no effect on the complex. In contrast, under similar conditions the thallium ion is removed from the Pt/Tl complex **2**.⁹

In attempts to carry out two-fragment, two-center oxidative addition to the Tl–Ir unit, $[\text{Tl}(\text{crown-P}_2)\text{Ir}(\text{CO})\text{Cl}]\text{NO}_3$ was oxidized with molecular iodine and phenyl iodide dichloride (a synthon for dichlorine).²⁰ Addition of molecular iodine yields a bright orange adduct, $[\text{ITl}(\text{crown-P}_2)\text{Ir}(\text{CO})\text{I}](\text{NO}_3)$ (**7**). The increase in $\nu(\text{CO})$ from 1968 cm^{-1} in **5** to 2047 cm^{-1} (dichloromethane solution) in **7** is consistent with oxidative addition.¹⁷ The infrared spectrum also indicates that nitrate ion is present ($\nu(\text{NO})$, 1345 cm^{-1} in Nujol). The $^{31}\text{P}\{^1\text{H}\}$ NMR spectrum shows a doublet at 4.6 ppm with $^2J(\text{Tl,P}) = 419\text{ Hz}$. The increase in $^2J(\text{Tl,P})$ is remarkable. Reaction of $[\text{Tl}(\text{crown-P}_2)\text{Ir}(\text{CO})\text{Cl}](\text{NO}_3)$ with phenyl iodide dichloride yields a pale yellow adduct $[\text{CITl}(\text{crown-P}_2)\text{Ir}(\text{CO})\text{Cl}_2](\text{NO}_3)$ (**8**). Again the the infrared spectrum indicates that the iridium has undergone oxidation with $\nu(\text{CO}) = 2047\text{ cm}^{-1}$ (Nujol mull), and that the nitrate ion is present ($\nu(\text{NO}) = 1350\text{ cm}^{-1}$). The $^{31}\text{P}\{^1\text{H}\}$ NMR spectrum shows two similar doublets. The major species has $\delta = 8.4\text{ ppm}$ and $^2J(\text{Tl,P}) = 570\text{ Hz}$, while the minor has $\delta = 11.3\text{ ppm}$ and $^2J(\text{Tl,P}) = 590\text{ Hz}$. Both have similar solubilities, and an effective method of purification or separation has not been found. We suspect that the two are structural isomers. The use of different reaction conditions (lower or higher reaction temperature or use of dichlorine as the oxidant) always resulted in a smaller ratio of the two products than the 8:1 ratio observed with the procedure given in the Experimental Section.

The $^{13}\text{C}\{^1\text{H}\}$ NMR spectra of these crown- P_2 complexes are useful for their characterization. Moreover, they show novel coupling effects. Relevant data for the free ligand and complexes **6–8** are set out in Table I. Figure 2 shows the $^{13}\text{C}\{^1\text{H}\}$ NMR

(15) Van Vliet, P. I.; Vrieze, K. *J. Organomet. Chem.* **1977**, *139*, 337.
 (16) Young, J. F. *Adv. Inorg. Chem. Radiochem.* **1968**, *11*, 91. Zubieta, J. A.; Zuckerman, J. J. *Prog. Inorg. Chem.* **1978**, *24*, 251. Holt, M. S.; Wilson, W. L.; Nelson, J. H. *Chem. Rev.* **1989**, *89*, 11.
 (17) Vaska, L. *Acc. Chem. Res.* **1968**, *1*, 335.
 (18) Wang, H.-H.; Pignolet, L. H.; Reedy, P. E., Jr.; Olmstead, M. M.; Balch, A. L. *Inorg. Chem.* **1987**, *26*, 377.
 (19) Brady, R.; Flynn, B. R.; Goeffroy, G. L.; Gray, H. B.; Peone, J., Jr.; Vaska, L. *Inorg. Chem.* **1976**, *15*, 1485.

(20) Giandomenico, C. M.; Hanan, L. H.; Lippard, S. J. *Organometallics* **1982**, *1*, 142.

Table I. $^{13}\text{C}\{^1\text{H}\}$ NMR Data^a


| carbon | crown-P ₂ | | 6 | | 7 | | 8 | |
|--------|-------------------------------|----------------------|-------------------------------|----------------------|--|----------------------|--|----------------------|
| | $\delta(\text{CDCl}_3)$, ppm | $J(\text{P,C})$, Hz | $\delta(\text{CDCl}_3)$, ppm | $J(\text{X,C})$, Hz | $\delta(\text{CD}_2\text{Cl}_2)$, ppm | $J(\text{X,C})$, Hz | $\delta(\text{CD}_2\text{Cl}_2)$, ppm | $J(\text{X,C})$, Hz |
| a | 138.6 (d) | 13.6 | b | 53 (Tl) | b | 64 (Tl) | b | 82 (Tl) |
| b | 133.0 (d) | 17.4 | 134.8 (br, d) | | 135.6 (d, t) | 4 (P) | 135.1 (d, t) | 4 (P) |
| c | 128.3 (d) | 6.6 | 128.4 (d, t) | 36 (Tl) | 128.1 (d, t) | 195 (Tl) | 128.7 (d, t) | 170 (Tl) |
| d | 128.4 (s) | | 131.3 (d) | 30 (Tl) | 132.0 (d) | 5 (P) | 132.2 (d) | 5 (P) |
| e | 59.5 (d) | 5.3 | 52.2 (m) | 20 (Tl) | 65.4 (br, d) | 137 (Tl) | 66.2 (br, d) | 123 (Tl) |
| f | 55.0 (d) | 8.6 | 57.7 (d) | 15 (Tl) | 58.2 (s) | 28 (Tl) | 58.3 (s) | 41 (Tl) |
| g | 69.8 (s) | | 68.2 (d) | 10 (Tl) | 68.4 (s) | | 69.3 (s) | |
| h | 70.6 (s) | | 70.1 (d) | | 69.5 (s) | | 70.4 (s) | |

^a Abbreviations: d, doublet; br, broad; s, singlet; t, triplet. ^b Data collected too rapidly to observe quarternary carbons.

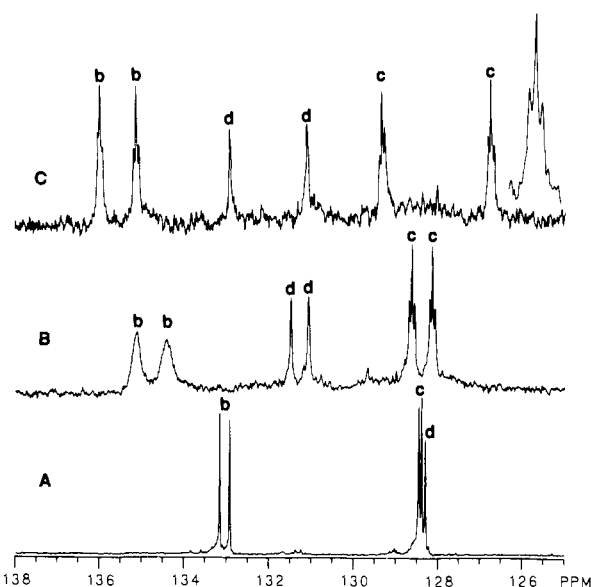


Figure 2. 75.44-MHz ^{13}C NMR spectra of (A) crown-P₂, (B) $[\text{Tl}(\text{crown-P}_2)\text{Ir}(\text{CO})\text{Cl}](\text{NO}_3)$ (**6**), and (C) $[\text{Ir}(\text{crown-P}_2)\text{Ir}(\text{CO})\text{Cl}](\text{NO}_3)$ (**7**) in dichloromethane solution at 23 °C. Labels b, c, and d identify the resonances of the ortho, meta, and para carbon atoms of the phenyl groups. The expansion at the upper right of trace C was made to emphasize the 1:2:1 triplet structure of the adjacent resonance.

spectra for the free ligand, **6**, and **7** in the region where the resonances of the phenyl groups appear. The spectrum of the free ligand shows the expected eight resonances in normal regions with coupling of phosphorus to the methylene carbons bound to nitrogen and all of the phenyl carbons except the ones in position d (Table I). The spectrum of the thallium/iridium complex **6** shows Tl–C coupling for carbon atoms within the crown ether portion and for carbon atoms of the phenyl ring. Notice that the coupling is 1.5–5 times greater for carbon atoms of the phenyl rings than for the aliphatic carbons despite the fact that the phenyl carbons are structurally quite remote from the site of the thallium ion within the complex. These couplings are readily seen in trace B of Figure 2. The resonances for the c carbons appear as a doublet (due to Tl–C coupling) of triplets (due to P–C coupling). The P–C coupling constants are similar in the free ligand and the complex. However, in the complex a triplet appears because of virtual coupling of the two trans phosphorus atoms. Such virtual coupling is, of course, absent in the free ligand where the P–Ir–P unit is lacking. The resonances of the d carbons in the complex (trace B) appear as a simple doublet since no coupling to the phosphorus

is resolved in either **6** or the free ligand. The resonances of the b carbons appear as a broad doublet (due to Tl–C coupling). The unusual breadth of these two resonances may result from unresolved P–C coupling (a triplet is expected for each of the two resonances). Oxidative addition of halogens to **6** increases the magnitude of the Tl–C coupling to the phenyl carbons but reduces the magnitude of coupling to the methylene carbons of the crown portion to the point where it is not detected. Resolution within the carbon of the P–C–N bridge becomes improved and the thallium–carbon coupling is observed there. These effects on the phenyl carbon resonances are readily seen by comparing traces B and C of Figure 2. The resonances of carbons b and c are doublets of triplets while for carbon d a simple doublet is observed. Previously values of $J(\text{Tl,C})$ in the 120–140-Hz range have been observed for aromatic carbon atoms of the anthracene ring of the thallium complexes of anthracene–cryptand ligands.²¹ These couplings were taken as evidence of bonding between the cation and the anthracene ring.²¹ However, the results shown in Figure 2 suggest that Tl–C coupling of a sizable magnitude can occur even to aromatic carbon atoms that are quite remote from the thallium ion itself and where no direct bonding exists.

As a model for the oxidative addition products, **7** and **8**, the Tl(II)–Ir(II) species $[(\text{CH}_3\text{CO}_2)_2\text{Tl}(\mu\text{-O}_2\text{CCH}_3)\text{Ir}(\text{CO})(\text{PPh}_3)_2(\text{O}_2\text{CCH}_3)]$ (**9**) reported by van Vliet and Vrieze was prepared by following a modification of their original procedure.¹⁵ This involves the addition of Tl(III) acetate to $\text{Ir}(\text{CO})\text{Cl}(\text{PPh}_3)_2$ in the presence of silver(I) acetate. The spectroscopic data already available from their report and reproduced by us show considerable similarity to that obtained for the diiodine and dichlorine addition products of $[\text{Tl}(\text{crown-P}_2)\text{Ir}(\text{CO})\text{Cl}](\text{NO}_3)$. Thus the $[(\text{CH}_3\text{CO}_2)_2\text{Tl}(\mu\text{-O}_2\text{CCH}_3)\text{Ir}(\text{CO})(\text{PPh}_3)_2(\text{O}_2\text{CCH}_3)]$ complex shows $\nu(\text{CO})$ at 2067 cm^{-1} (i.e. oxidized relative to a $\text{IrI}(\text{CO})\text{ClP}_2$ unit) and a large value for $^2J(\text{Tl,P})$ (1119 Hz). We believe that all these species (**7**, **8**, and **9**) contain normal Tl(II)–Ir(II) single bonds. In viewing **9** as a model for the oxidative-addition products **7** and **8** it is interesting to note the variation in colors; **9**, white; **7**, orange, and **8**, pale yellow. This variation is probably due to the presence of halide to metal charge transfer bands in **7** and **8** and their absence in white **9**. The structure of the acetate-bridged complex is reported in a subsequent section. For comparison the structure of $[\text{TlIr}_2(\text{CO})_2\text{Cl}_2(\mu\text{-dpma})_2](\text{NO}_3)$ (**4**) obtained as described previously¹⁴ is also considered.

The Crystal and Molecular Structure of $[\text{Tl}(\text{crown-P}_2)\text{Ir}(\text{CO})\text{Cl}](\text{NO}_3)\cdot\text{CH}_2\text{Cl}_2$ (6**).** The asymmetric unit consists of one complex cation, a normal planar nitrate, and a molecule of di-

(21) Fages, F.; Desvergne, J.-P.; Bouas-Laurent, H.; Marsau, P.; Lehn, J.-M.; Kotzyba-Hibert, F.; Albrecht-Gary, A.-M.; Al-Joubbeh, M. *J. Am. Chem. Soc.* **1989**, *111*, 8672.

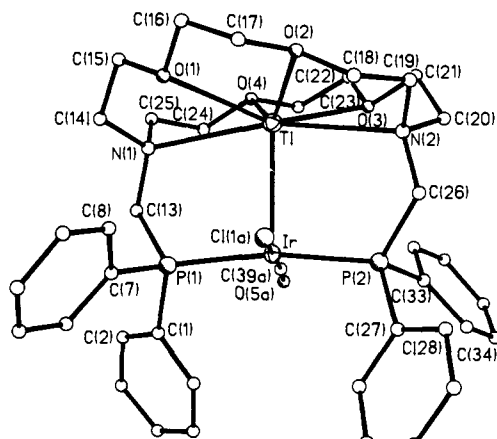


Figure 3. A view of the cation in $[\text{Tl}(\text{crown-P}_2)\text{Ir}(\text{CO})\text{Cl}](\text{NO}_3)\cdot\text{CH}_2\text{Cl}_2$ (**6**) with 50% thermal contours for iridium and thallium and uniform, arbitrarily-sized circles for other atoms.

Table II. Selected Interatomic Distances and Angles in $[\text{Tl}(\text{crown-P}_2)\text{Ir}(\text{CO})\text{Cl}](\text{NO}_3)\cdot\text{CH}_2\text{Cl}_2$

| Distances (Å) | | | | | |
|---------------------|-----------|-----------------|-----------|-----------|-----------|
| At Ir | | | | | |
| Ir-Tl | 2.875 (1) | Ir-P(2) | 2.321 (3) | Ir-C(39B) | 1.82 |
| Ir-P(1) | 2.327 (3) | Ir-Cl(1A) | 2.403 (5) | Ir-C(39B) | 1.89 |
| | | Ir-Cl(1B) | 2.410 (7) | | |
| At Tl | | | | | |
| Tl-Ir | 2.875 (1) | Tl-O(2) | 2.810 (8) | Tl-N(1) | 2.965 (9) |
| Tl-O(1) | 2.880 (8) | Tl-O(3) | 2.834 (8) | Tl-N(2) | 2.985 (9) |
| | | Tl-O(4) | 2.836 (8) | | |
| Angles (deg) | | | | | |
| At Ir | | | | | |
| P(1)-Ir-P(2) | 169.5 (1) | P(2)-Ir-C(39A) | 94.2 (5) | | |
| Cl(1A)-Ir-C(39A) | 176.4 (7) | Tl-Ir-P(1) | 95.2 (1) | | |
| P(1)-Ir-Cl(1A) | 93.6 (2) | Tl-Ir-P(2) | 95.3 (1) | | |
| P(1)-Ir-C(39A) | 85.5 (5) | Tl-Ir-Cl(1A) | 87.0 (1) | | |
| P(2)-Ir-Cl(1A) | 83.4 (2) | Tl-Ir-C(39A) | 95.9 (3) | | |
| At Methylene Bridge | | | | | |
| P(1)-C(13)-N(1) | 115.3 (8) | P(2)-C(26)-N(2) | 116.9 (8) | | |
| At Tl | | | | | |
| O(1)-Tl-O(2) | 60.9 (4) | N(2)-Tl-O(2) | 63.6 (4) | | |
| O(1)-Tl-O(3) | 152.1 (4) | N(2)-Tl-O(3) | 62.2 (4) | | |
| O(1)-Tl-O(4) | 107.5 (4) | N(2)-Tl-O(4) | 122.9 (4) | | |
| O(2)-Tl-O(3) | 108.6 (4) | N(1)-Tl-N(2) | 165.2 (4) | | |
| O(2)-Tl-O(4) | 136.7 (4) | Ir-Tl-N(1) | 82.4 (1) | | |
| O(3)-Tl-O(4) | 60.7 (4) | Ir-Tl-N(2) | 82.8 (1) | | |
| N(1)-Tl-O(1) | 60.9 (4) | Ir-Tl-O(1) | 104.0 (1) | | |
| N(1)-Tl-O(2) | 121.8 (4) | Ir-Tl-O(2) | 111.5 (1) | | |
| N(1)-Tl-O(3) | 122.8 (4) | Ir-Tl-O(3) | 103.9 (1) | | |
| N(1)-Tl-O(4) | 64.2 (4) | Ir-Tl-O(4) | 111.8 (1) | | |
| N(2)-Tl-O(1) | 122.4 (4) | | | | |

chloromethane with no unusual contacts between these units. A view of the cation is given in Figure 3. Interatomic distances and angles are collected in Table II.

The cation consists of a thallium ion encapsulated within the aza-crown portion and the iridium ion bonded to the two phosphorus atoms of the crown- P_2 . The iridium ion has the usual trans-planar array of phosphine, carbonyl, and chloride ligands. As is typical for such complexes, there is disorder between the positions of the carbonyl and chloride ligand.²² The predominant form, which occurs at 60% occupancy, is shown in the figure; the other form simply has these two ligands interchanged. While the bond distances within the $\text{IrP}_2\text{Cl}(\text{CO})$ unit are entirely normal,

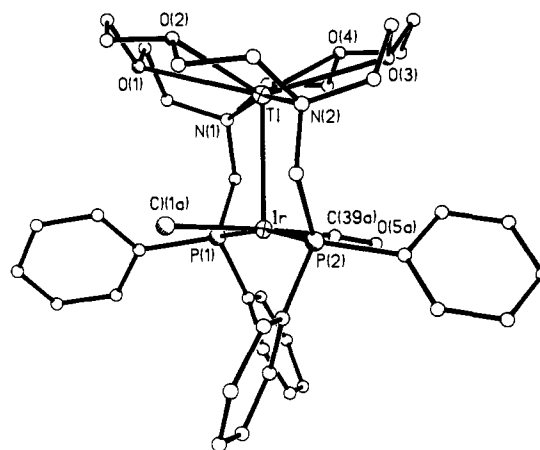


Figure 4. A view of $[\text{Tl}(\text{crown-P}_2)\text{Ir}(\text{CO})\text{Cl}]^+$ that emphasizes its approximation to 2-fold rotational symmetry.

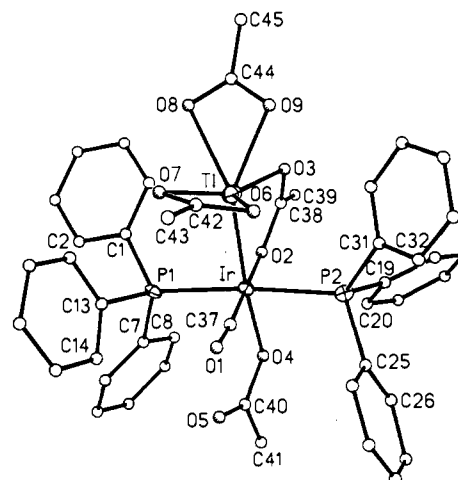


Figure 5. A drawing of the structure of $(\text{CH}_3\text{CO}_2)_2\text{Tl}(\mu\text{-O}_2\text{CCH}_3)\text{Ir}(\text{CO})(\text{PPh}_3)_2(\text{O}_2\text{CCH}_3)$ (**9**), with 50% thermal contours for iridium, thallium, and phosphorus and uniform, arbitrarily-sized circles for carbon and oxygen.

and similar to those of other Vaska-like complexes,²² the *trans*-P(1)-Ir-P(2) unit is not linear (the angle is $169.5(12)^\circ$) but is bent in the direction that allows the iridium to be close to the thallium ion. The Tl-Ir distance, 2.875 (1) Å, is indicative of bonding between these entities. For comparison the Tl-Pt distances in **2** are slightly longer (2.911 (2) and 2.958 (2) Å) for the two crystallographically independent cations in the crystal used for the structure determination. The thallium ion is centered over the iridium coordination plane with Tl-Ir-ligand angles near 90° . While the complex itself has no crystallographically-imposed symmetry, the $\text{Tl}(\text{crown-P}_2)\text{Ir}$ portion (without the carbonyl and chloride ligands) has approximate C_2 symmetry with the C_2 axis passing through the iridium and thallium ions. Figure 4 shows the cation from a perspective that emphasizes this pseudosymmetry.

The geometry of the thallium ion within the aza-crown portion is similar to that seen in related compounds containing thallium in similar environments.^{23,24} The Tl-O distances average 2.840 Å and span a narrow range (2.810–2.880 Å). These are shorter than the Tl-N distances, 2.965 (9) and 2.985 (9) Å. Note that the Tl-Ir distance is just slightly longer than the Tl-O distances, but shorter than the Tl-N distances. Since the covalent radius of iridium is much larger than that of oxygen or nitrogen, there can be no question that significant bonding between thallium and iridium is present in this complex.

(22) Brady, R.; DeCamp, W. H.; Flynn, B. R.; Schneider, M. L.; Scott, J. D.; Vaska, L.; Werneke, M. F. *Inorg. Chem.* **1975**, *14*, 2669.

(23) Moras, D.; Weiss, R. *Acta Crystallogr.* **1973**, *B29*, 1059.

(24) Faggiani, R.; Brown, I. D. *Acta Crystallogr.* **1982**, *B38*, 2473.

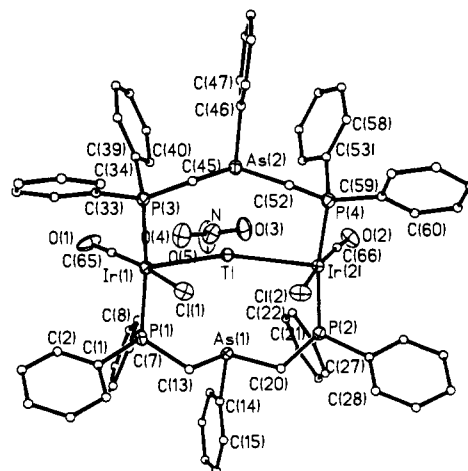
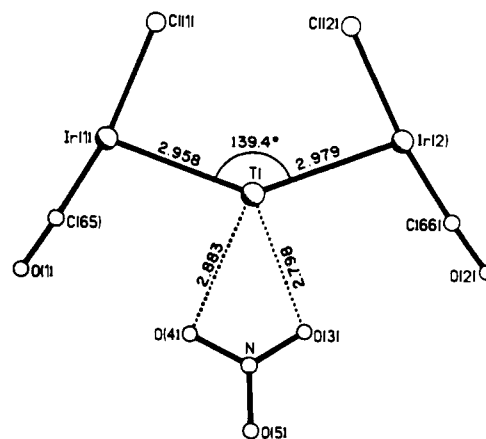
Table III. Selected Interatomic Distances and Angles in $(\text{CH}_3\text{CO}_2)_2\text{Tl}(\mu\text{-O}_2\text{CCH}_3)\text{Ir}(\text{CO})(\text{PPh}_3)_2(\text{O}_2\text{CCH}_3)\cdot\text{CHCl}_3$

| Distances (Å) | | | | | |
|---------------|-----------|----------------|------------|----------|------------|
| At Ir | | | | | |
| Ir–Tl | 2.611 (1) | Ir–P(2) | 2.395 (5) | Ir–O(4) | 2.081 (12) |
| Ir–P(1) | 2.378 (5) | Ir–O(2) | 2.097 (15) | Ir–C(73) | 1.86 (2) |
| At Tl | | | | | |
| Tl–Ir | 2.611 (1) | Tl–O(4) | 2.47 (2) | Tl–O(8) | 2.45 (2) |
| Tl–O(3) | 2.87 (2) | Tl–O(7) | 2.37 (2) | Tl–O(9) | 2.24 (1) |
| Angles (deg) | | | | | |
| About Ir | | | | | |
| Tl–Ir–P(1) | 93.3 (1) | P(1)–Ir–C(37) | 92.5 (6) | | |
| Tl–Ir–P(2) | 93.3 (1) | P(2)–Ir–O(2) | 90.9 (3) | | |
| Tl–Ir–C(37) | 83.4 (5) | P(2)–Ir–C(37) | 89.6 (6) | | |
| Tl–Ir–O(2) | 97.0 (3) | O(4)–Ir–P(1) | 90.3 (4) | | |
| Tl–Ir–O(4) | 174.9 (3) | O(4)–Ir–P(2) | 83.1 (4) | | |
| P(1)–Ir–P(2) | 173.3 (2) | O(4)–Ir–O(2) | 79.6 (5) | | |
| O(2)–Ir–C(37) | 179.3 (6) | O(94)–Ir–C(37) | 100.0 (7) | | |
| P(1)–Ir–O(2) | 86.9 (3) | | | | |
| About Tl | | | | | |
| Ir–Tl–O(3) | 73.5 (4) | O(3)–Tl–O(9) | 75.0 (6) | | |
| Ir–Tl–O(6) | 108.1 (3) | O(6)–Tl–O(7) | 54.5 (5) | | |
| Ir–Tl–O(8) | 116.9 (3) | O(6)–Tl–O(8) | 120.3 (5) | | |
| Ir–Tl–O(9) | 130.6 (4) | O(6)–Tl–O(9) | 86.1 (5) | | |
| O(3)–Tl–O(6) | 143.8 (4) | O(7)–Tl–O(8) | 86.0 (5) | | |
| O(3)–Tl–O(7) | 141.5 (6) | O(7)–Tl–O(9) | 98.6 (5) | | |
| O(3)–Tl–O(8) | 160.0 (6) | O(8)–Tl–O(9) | 54.5 (5) | | |
| O(3)–Tl–O(9) | 74.8 (6) | | | | |

The Crystal and Molecular Structure of $[(\text{CH}_3\text{CO}_2)_2\text{Tl}(\mu\text{-O}_2\text{CCH}_3)\text{Ir}(\text{CO})(\text{PPh}_3)_2(\text{O}_2\text{CCH}_3)]\cdot\text{CH}_2\text{Cl}_2$ (9). The asymmetric unit consists of the binuclear complex and a molecule of dichloromethane with no unusual intermolecular contacts. The structure of the complex is shown in Figure 5. Selected interatomic distances and angles are presented in Table III.

The complex consists of a six-coordinate iridium bound to a six-coordinate thallium through a Tl–Ir bond and a bridging acetate. The Tl–Ir bond length of 2.611 (1) Å is considerably shorter than the Tl–Ir distance in **6** (2.875 (1) Å). The two triphenylphosphine ligands on iridium have the unusual trans orientation. The carbonyl group is trans to the bridging acetate, while the other acetate ligand is trans to the thallium ion. That acetate is monodentate, the Ir...O(5) distance (3.15 (1) Å) is too long for bonding. The geometry at iridium is octahedral-like with cis bond angles comprising a narrow range (79.6–100.0°) that is near 90° and nearly linear trans angles. In marked contrast, the angular distribution of ligands about thallium does not assume any particular pattern. There is a wide range of interligand angles about thallium with the chelating O–Tl–O angle of 54.5 (5)° as the narrowest. The range of Tl–O distances is quite large. For the chelating acetate ligands the range is 2.24 (1)–2.47 (2) Å, while the Tl–O distance (2.87 (2) Å) involving the bridging acetate is much longer. In thallium(III) acetate monohydrate there is also a wide spread of Tl–O distances (2.17 (1)–2.78 (2) Å).²³ It is interesting to note that the Tl–Ir complex in Figure 5 contains all three bonding modes that are common for acetate anion: chelating, bridging, and monodentate.

The Structure of $\text{Ir}_2\text{Tl}(\text{NO}_3)(\text{CO})_2\text{Cl}_2(\mu\text{-dpma})_2$ (4). The structure of this complex is shown in Figure 6. Some dimensions within the central core are shown in Figure 7. The thallium ion is bonded to the metallomacrocycle through two Tl–Ir bonds which are nearly equal in length (2.958 (1) and 2.979 (1) Å). These are longer than the Tl–Ir bond lengths in **6** (2.875 (1) Å) or **9** (2.611 (1) Å). The Tl...As distances (3.295 (3) and 3.308 (3) Å) are too long for them to be considered as bonded. The Tl–O(3) and Tl–O(4) distances (2.80 (1) and 2.99 (1) Å) are somewhat unsymmetrical. They are comparable to the Tl–O distances seen in the crown- P_2 complex, **6**, but somewhat longer than the Tl–O distances seen in the acetate complex, **9**, where thallium is formally in a higher oxidation state. The nitrate ion is slightly tipped with

**Figure 6.** The structure of $\text{Ir}_2\text{Tl}(\text{NO}_3)(\text{CO})_2\text{Cl}_2(\mu\text{-dpma})_2$.**Figure 7.** A view of the $[\text{Ir}(\text{CO})\text{Cl}]_2\text{TlNO}_3$ core of $\text{Ir}_2\text{Tl}(\text{NO}_3)(\text{CO})_2\text{Cl}_2(\mu\text{-dpma})_2$.

respect to the Ir_2Tl plane. Crystallographic data are given in the supplementary material that accompanies ref 14.

Discussion

The structures described here show that significant bonding between thallium and iridium is possible. Complexes **4** and **6**, which involve combinations of Ir(I) and Tl(I), have relatively long bonds in the 2.85–3.00-Å range, which is consistent with the low formal bond order involved. In the acetate-bridged complex **9**, however, where there is a formal Tl–Ir single bond, the Tl–Ir bond is considerably shortened. This bond shortening and strengthening is also accompanied by an increase in the magnitude of the Tl–P coupling as seen in the ^{31}P NMR spectrum. We take such an increase in this two-bond coupling to be indicative of bond strengthening and note that similar changes are observed when the P_2 -crown complex **6** undergoes oxidative addition of halogen. Although oxidative additions to d^8 – d^8 transition-metal dimers are fairly common,²⁵ the results described here are the first example of oxidative addition to a main-group-metal/transition-metal, s^2 – d^8 assembly. These oxidative addition reactions are accompanied by an increase in the $\text{C}\equiv\text{O}$ stretching frequency for the carbon monoxide ligands. The acetate bridged complex **9** has a $\text{C}\equiv\text{O}$ stretching frequency that is comparable to those of the oxidative-addition products **7** and **8**. Complex **9** in turn may be viewed as the product of oxidative addition of a Tl(III) acetate unit to its Ir(I) precursor. The structure of **9** shows a six-coordinate iridium whose geometry is consistent with oxidation at that site. Precedent for this sort of oxidative addition of a metal–ligand bond

(25) Mann, K. R.; Gordon, J. G., II; Gray, H. B. *J. Am. Chem. Soc.* **1975**, *97*, 3553. Balch, A. L. *J. Am. Chem. Soc.* **1976**, *98*, 8049. Fordyce, W. A.; Crosby, G. A. *J. Am. Chem. Soc.* **1982**, *104*, 985.

Table IV. Crystal Data, Data Collection, and Structure Solution Parameters for [Tl(crown-P₂)Ir(CO)Cl](NO₃)·CH₂Cl₂ (**6**) and (CH₃CO)₂Tl(μ-O₂CCH₃)Ir(CO)(PPh₃)₂(O₂CCH₃)·CHCl₃ (**9**)

| | [Tl(crown-P ₂)Ir(CO)Cl](NO ₃)·CH ₂ Cl ₂ | (CH ₃ CO) ₂ Tl(μ-O ₂ CCH ₃)Ir(CO)(PPh ₃) ₂ (O ₂ CCH ₃)·CHCl ₃ |
|---|---|---|
| formula | C ₄₀ H ₅₀ Cl ₃ IrN ₃ O ₈ P ₂ Tl | C ₄₆ H ₄₃ Cl ₃ IrO ₉ P ₂ Tl |
| fw | 1265.76 | 1304.75 |
| color and habit | yellow-orange needles | colorless plates |
| crystal system | triclinic | monoclinic |
| space group | P $\bar{1}$ (No. 2) | P2 ₁ /c (No. 14) |
| a, Å | 11.350 (4) | 10.815 (3) |
| b, Å | 13.519 (4) | 22.909 (8) |
| c, Å | 15.022 (4) | 21.582 (7) |
| α, deg | 97.64 (2) | |
| β, deg | 101.20 (3) | 118.63 (2) |
| γ, deg | 93.63 (3) | |
| V, Å ³ | 2231 (1) | 4693 (2) |
| T, K | 130 | 130 |
| Z | 2 | 4 |
| cryst dimens, mm | 0.10 × 0.25 × 0.50 | 0.05 × 0.18 × 0.28 |
| d _{calcd} , g cm ⁻³ | 1.88 | 1.85 |
| radiation, Å | Mo Kα (λ = 0.71069) | Mo Kα (λ = 0.71069) |
| μ(Mo Kα), cm ⁻¹ | 70.9 | 67.4 |
| range of transmission factors | 0.21–0.56 | 0.35–0.75 |
| diffractometer | P2 ₁ , graphite monochromator | P2 ₁ , graphite monochromator |
| scan method | ω, 1.0° range, 1.0° offset for bkgnd | ω, 1.4° range, 1.0° offset for bkgnd |
| scan speed, deg min ⁻¹ | 15 | 10 |
| 2θ range, deg | 0–50 | 0–45 |
| octants collected | h, ±k, ±l | h, k, ±l |
| no. of data collected | 7845 | 6641 |
| no. of unique data | 7845 | 6073 [R(merge) = 0.040] |
| no. of data used in refinement | 6298 (I > 2σ(I)) | 3961 (I > 2σ(I)) |
| no. of parameters refined | 243 | 296 |
| R ^a | 0.070 | 0.063 |
| R _w ^a | 0.078 [w = 1/σ ² (F _o)] | 0.059 [w = 1/σ ² (F _o)] |

$$^a R = \sum ||F_o| - |F_c|| / \sum |F_o| \text{ and } R_w = \sum ||F_o| - |F_c|| w^{1/2} / \sum |F_w w^{1/2}|.$$

to an Ir(I) complex is seen in the many additions of mercuric halides to d⁸ metal complexes which results in the formation of mercury–transition-metal bonds.²⁶ The presence of the bridging acetate in **9** was unexpected since the original infrared work was interpreted to indicate that all carboxylate groups were terminal.¹⁵

The Tl–Ir bonding within **6** should be viewed in light of the theoretical work on Tl₂Pt(CN)₄.⁸ In that complex bonding between the Pt(CN)₄²⁻ and the thallium(I) is found to be largely electrostatic, but there is also substantial contribution from covalent interactions. These involve interactions of the filled 5d_{z²} orbital of platinum, the filled 6s orbital on thallium, and the empty p_z orbitals on each metal. For **6**, then, the iridium-filled 5d_{z²} and empty p_z orbitals are utilized similarly. The degree of ionic bonding may be reduced since the IrP₂(CO)Cl fragment is uncharged. The absorption seen at 400 nm may be the counterpart of the σ* → σ band seen for d⁸–d⁸ platinum metal dimers.²⁵ However, relativistic effects²⁷ play a significant role in making accurate spectroscopic assignments.⁸ Consequently thorough analysis of the electronic absorption and emission spectrum of **6** must await theoretical calculations and further experimental study. However, it does appear that the luminescence seen at 77 K results from phosphorescence that is pumped by both the spin-allowed and spin-forbidden transitions seen in the absorption spectrum.

The difference in coordination environments for iridium and thallium in complexes **4**, **6**, and **9** is striking. In each iridium has rectangular geometry with cis bond angles very near 90° and spanning a relatively narrow range. The iridium coordination number in **4** and **6** is five while when oxidized (in **9**) it increases to six. On the other hand thallium possesses a much more plastic environment. Its coordination number in **4** is four, in **6** it is seven, and in **9** it is six. As expected for cases where the metal–ligand interactions are largely electrostatic, the angular disposition of the ligands about thallium is also highly variable.

Experimental Section

Preparation of Compounds. Samples of Ir(CO)₂Cl(*p*-tolNH₂),²⁸ iodobenzene dichloride,²⁹ and crown-P₂⁹ were obtained as described previously.

[Tl(crown-P₂)Ir(CO)Cl] (5). A solution of Ir(CO)₂Cl(*p*-toluidine) (100 mg, 0.26 mmol) in dry toluene (17 mL) was slowly added to a stirred suspension of crown-P₂ (168 mg, 0.26 mmol) in dry toluene (6 mL) over a period of 1 h. After being stirred for 1 h, the clear yellow solution was evaporated to dryness. Addition of diethyl ether to the resulting yellow-brown oil gave **1** as a dark-yellow, air-sensitive solid (yield: 180 mg; 77%). Anal. Calcd for C₃₉H₄₈ClIrN₂O₃P₂: C, 51.22; H, 5.29; N, 3.06. Found: C, 50.16; H, 5.34; N, 2.90.

[Tl(crown-P₂)Ir(CO)Cl](NO₃) (6). A solution of Ir(CO)₂Cl(*p*-toluidine) (90 mg, 0.230 mmol) in toluene (30 mL) was added to a stirred suspension of crown-P₂ (150 mg, 0.230 mmol) in toluene (10 mL) over a period of 1 h. The resulting bright-yellow, air-sensitive solution was evaporated to dryness under reduced pressure. The yellow-brown oily product was redissolved in CH₂Cl₂ (10 mL) and solid thallium(I) nitrate (120 mg, 0.450 mmol) was added to the stirred solution. A dark-orange mixture was obtained within 10 min. After being stirred for 1 h, the solution was filtered to remove unreacted thallium(I) nitrate. Dropwise addition of diethyl ether to the clear orange solution gave a precipitate of the product as air-stable, yellow-orange needles (yield: 215 mg; 80%).

[Tl(crown-P₂)Ir(CO)Cl](NO₃) (7). A solution of I₂ (17.8 mg, 0.070 mmol) in CH₂Cl₂ (3 mL) was added to a stirred yellow-orange solution of [Ir(CO)Cl(P₂-crown)Tl](NO₃) (80 mg, 0.068 mmol) in CH₂Cl₂ (1 mL). Immediately, the solution turned dark orange. After being stirred for 20 min, the solution was concentrated and diethyl ether added to give a bright orange solid, which was filtered off, washed with diethyl ether, and vacuum dried (yield: 90 mg; 93%). Anal. Calcd for C₃₉H₄₈ClI₂IrN₃O₈P₂Tl: C, 32.65; H, 3.37; N, 2.93; P, 4.32. Found: C, 32.55; H, 3.21; N, 2.54; P 4.02.

[Tl(crown-P₂)Ir(CO)Cl₂](NO₃) (8). The complex [Ir(CO)ClTl(crown-P₂)](NO₃) (78 mg, 0.066 mmol) was dissolved in CH₂Cl₂ (5 mL), and the yellow-orange solution was cooled to –50 °C (dry ice–acetone bath). Solid phenyl iodide dichloride (18 mg, 0.066 mmol) was then added in one portion with stirring. The solution turned pale yellow in a few seconds. After 20 min, the solution was allowed to warm to room

(26) Brotherton, P. D.; Raston, C. L.; White, A. H.; Wild, S. B. *J. Chem. Soc.* **1976**, 1799.

(27) Pyykkö, P.; Desclaux, J. P. *Acc. Chem. Res.* **1979**, *12*, 276; Pitzer, K. *Acc. Chem. Res.* **1979**, *12*, 271. Pyykkö, P. *Chem. Rev.* **1988**, *88*, 563.

(28) Klabunde, U. *Inorg. Synth.* **1974**, *15*, 82.

(29) Lucas, H. J.; Kennedy, E. R. *Org. Synth.* **1955**, *Collect. Vol.* **3**, 482.

temperature. Diethyl ether was added, and the mixture was cooled to $-20\text{ }^{\circ}\text{C}$. A pale-yellow solid precipitated after standing overnight. This product was filtered off, washed with diethyl ether, and dried in vacuo (yield: 68 mg; 82%). Anal. Calcd for $\text{C}_{39}\text{H}_{48}\text{Cl}_3\text{IrN}_3\text{O}_8\text{P}_2\text{Ti}$: C, 37.42; H, 3.87; N, 3.36; Cl, 8.50. Found: C, 36.64; H, 3.81; N, 3.04; Cl, 7.60.

$[\text{Ir}(\text{PPh}_3)_2(\text{AcO})(\text{CO})(\mu\text{AcO})\text{Ti}(\text{AcO})_2]$. The complex has been prepared following modification of the original procedure.¹⁵ A 30-mg sample of $\text{Ag}(\text{CH}_3\text{COO})$ (0.179 mmol) was added to a suspension of $\text{Ir}(\text{CO})\text{Cl}(\text{PPh}_3)_2$ (140 mg, 0.179 mmol) in dry CH_2Cl_2 (8 mL) and the reaction mixture was rapidly stirred for 5 min in the dark. Solid $\text{Ti}(\text{C}-\text{H}_3\text{COO})_3 \cdot 1.5\text{H}_2\text{O}$ (73 mg, 0.179 mmol) was then added to the yellow suspension. Immediately the suspension turned deep orange (not red as previously reported). A clear orange solution was obtained after approximately 30 min. After being stirred for 1.5 h, the solution turned yellow, and after 3 h (overall reaction time) a white solid (AgCl) was removed by filtration. Hexane (15 mL) was then added to the yellow filtrate, and the mixture was cooled to $-20\text{ }^{\circ}\text{C}$. A cream microcrystalline solid precipitated overnight (yield: 71 mg; 33%). Further workup on the mother liquor gave another crop of the same product (yield: 43 mg; 20%).

X-ray Data Collection. $[\text{Ti}(\text{crown-P}_2)\text{Ir}(\text{CO})\text{Cl}](\text{NO}_3)$ (**5**). Yellow-orange crystals were obtained by slow diffusion of diethyl ether into a dichloromethane solution of the complex. They were coated with a light hydrocarbon oil to prevent cracking upon exposure to air. The crystal was mounted on a glass fiber with silicon grease and placed into the 130 K nitrogen stream of a Syntex P2₁ diffractometer with a modified LT-1 low-temperature apparatus. The space group was determined to be $P\bar{1}$. The two-check reflection showed only random fluctuations (<2%) in intensity throughout the data collection. The data were corrected for Lorentz and polarization effects. Crystal data are given in Table IV.

$(\text{CH}_3\text{CO}_2)_2\text{Ti}(\mu\text{-O}_2\text{CCH}_3)\text{Ir}(\text{CO})(\text{PPh}_3)_2(\text{O}_2\text{CCH}_3)\text{-CHCl}_3$. Colorless plates were obtained by slow diffusion of ethyl ether into a chloroform solution of the complexes. These were handled as described above for **5**. There was no decay in the intensity of two-check reflections during data collection.

Solution and Refinement of Structures. $[\text{Ti}(\text{crown-P}_2)\text{Ir}(\text{CO})\text{Cl}](\text{NO}_3) \cdot \text{CH}_2\text{Cl}_2$. The structure was solved by Patterson and difference Fourier methods. Computer programs are from SHELTL, Version 5, installed on a Data General Eclipse computer. Neutral atom scattering factors and corrections for anomalous dispersion are from a standard source.³⁰ The disorder in the carbonyl group and chloride bonded to Ir was modeled by assigning 60% weight to one arrangement (A) and 40% weight to the other (B). The positional parameters for the carbonyl

groups were taken from a final difference map and fixed. Thermal parameters for all the atoms in question were allowed to refine and are reasonable for the model. Hydrogen atoms were included at calculated positions with use of a riding model and C-H distances of 0.96 Å. The thermal parameters for the hydrogen atoms were fixed at 1.2 times the thermal parameter of the bonded carbon. An absorption correction was applied.³ Final refinement was carried out with anisotropic thermal parameters for Ir and Ti atoms. The largest peak in a final difference map had a value of $4.6\text{ e } \text{Å}^{-3}$, located 0.81 Å from Ti.

$(\text{CH}_3\text{CO}_2)_2\text{Ti}(\mu\text{-O}_2\text{CCH}_3)\text{Ir}(\text{CO})(\text{PPh}_3)_2(\text{O}_2\text{CCH}_3)\text{-CHCl}_3$. The structure was solved by Patterson and difference Fourier methods. Hydrogen atoms were included at calculated positions with use of a riding model and C-H distances of 0.96 Å. The thermal parameters for the hydrogen atoms were fixed at 1.2 times the equivalent isotropic thermal parameter of the bonded carbon. An absorption correction was applied.³¹ Final refinement was carried out with anisotropic thermal parameters for Ir, Ti, P, and Cl atoms. The largest peak in the final difference map had a value of $1.60\text{ e } \text{Å}^{-3}$ and was located 0.85 Å from Ir.

Physical Measurements. The $^{31}\text{P}\{^1\text{H}\}$ NMR spectra were recorded on a General Electric QE-300 NMR spectrometer that operates at 121.4 MHz with an external 85% phosphoric acid standard and the high field positive convention for reporting chemical shifts. Infrared spectra were recorded on an IBM IR32 spectrometer. Electronic spectra were recorded with a Hewlett-Packard 8450A spectrometer. Uncorrected emission spectra were obtained through the use of a Perkin-Elmer MPF-44B fluorescence spectrometer.

Acknowledgment. We thank the National Science Foundation (CHE-894209) for support, CNR/NATO for a fellowship to F.N., Dr. P. E. Reedy, Jr., for preparation of **4**, and Johnson Matthey, Inc. for a loan of iridium salts. The diffraction and computing equipment used in this study were purchased under NSF Grant CHE-8802721 to the University of California, Davis.

Supplementary Material Available: Tables of atomic coordinates, bond distances, bond angles, anisotropic thermal parameters, hydrogen atom positions, and crystal refinement data for **6** and **9** (10 pages); listings of observed and calculated structure factors (62 pages). Ordering information is given on any current masthead page.

(31) The method obtains an empirical absorption tensor from an expression relating F_o and F_c . Moezzi, B. Ph.D. Thesis, University of California, Davis, 1987.

(30) *International Tables of X-ray Crystallography*; Kynoch Press: Birmingham, England, 1974; Vol. 4.

Chromium(VI) Forms a Thiolate Complex with Glutathione

Samuel L. Brauer and Karen E. Wetterhahn*

Contribution from the Department of Chemistry, Dartmouth College, Hanover, New Hampshire 03755. Received July 5, 1990

Abstract: Reaction of potassium dichromate with the tripeptide glutathione resulted in the formation of a 1:1 complex of Cr^{VI} with glutathione. The red Cr^{VI} -glutathione adduct was stable for ~ 60 min at $4\text{ }^{\circ}\text{C}$ and $I = 1.5\text{ M}$. ^1H , ^{13}C , and ^{17}O NMR studies showed that glutathione acts as a monodentate ligand and binds to Cr^{VI} through the cysteinyl thiolate group, forming a GSCrO_3^- complex. No evidence was obtained for involvement of the other possible ligating groups, e.g., glutamyl amino and carboxylate, glycyl carboxylate, or peptide backbone, in binding to Cr^{VI} ; however, Cr^{VI} -induced conformational changes in the glutamyl and cysteinyl side chains of the tripeptide. EPR studies showed that two chromium(V) species ($g = 1.987$ and $g = 1.973$) are formed upon reaction of potassium dichromate with glutathione. Chromium-glutathione complexes may be involved in producing the high levels of chromium(VI)-induced DNA damage in cells having high concentrations of glutathione and may play an important role in the carcinogenicity of chromium(VI) compounds.

Introduction

Chromium(VI) compounds have been shown to be human carcinogens in several epidemiological studies.¹⁻³ Chromium(VI) toxicity and mutagenicity has been the subject of a recent review.⁴

In contrast, chromium(III) compounds are relatively nontoxic and noncarcinogenic. However, chromium(VI) does not react with

* To whom correspondence should be addressed: Department of Chemistry, Steele Hall, Dartmouth College, Hanover, NH 03755.

(1) *Chromium: Metabolism and Toxicity*; Burrows, D., Ed.; CRC Press: Boca Raton, FL, 1983.

(2) Levis, A. G.; Bianchi, V. In *Biological and Environmental Aspects of Chromium*; Langard, S., Ed.; Elsevier Biomedical Press: Amsterdam, 1982.